Research Article

Jianmeng Jiao*, Sethulakshmy Jayakumari, Maria Wallin, and Merete Tangstad

Graphite crucible interaction with Fe–Si–B phase change material in pilot-scale experiments

https://doi.org/10.1515/htmp-2022-0288
received March 23, 2023; accepted August 22, 2023

Abstract: Fe–26Si–9B alloy is a promising high temperature phase change material (HTPCM), due to its high heat of fusion, small volumetric change, abundance, and low cost. Additionally, graphite has been identified as a promising candidate for use as a container material for this alloy. In this study, the feasibility of using graphite for Fe–26Si–9B HTPCM is investigated in a pilot-scale. Specifically, 4–5 kg Fe–26Si–9B master alloys were melted in graphite crucibles using an induction furnace, which underwent 2–3 thermal cycles in the temperature range of 1,100–1,375°C. The results showed that SiC and B_4C precipitates were formed in the alloys. However, these carbides were found to be present only on the surface of the solidified alloys and not in the main body. Still, the chemical composition of the Fe–26Si–9B alloy remained relatively stable during the thermal cycles. It was also seen that the graphite crucible withstood the temperature cycles without cracking. Therefore, the use of graphite as a container for Fe–26Si–9B phase change material is a promising approach.

Keywords: Fe–Si–B, thermal cycle, pilot scale, graphite, HTPCM

1 Introduction

Renewable energies, such as solar and wind power, play a crucial role in reducing greenhouse emissions and an increasing demand of green energy is expected in the coming decades. Solar power is anticipated to become the largest source of installed capacity by 2035, while wind power capacity is expected to triple by 2040 compared to 2020 [1]. However, their intermittent nature presents a challenge as energy supply does not always match energy demand. To address this issue, thermal energy storage (TES) techniques have been developed. These techniques enable the storage of renewable energy at the time it is produced and release the stored energy for later use. Among the various TES techniques, phase change material (PCM) has emerged as one of the most promising options.

PCM is a material that can store and release energy through phase changes without significant changes in temperature. Among the PCMs, metallic materials have been identified as the potential high temperature phase change material (HTPCM) in the TES system, owing to their high thermal conductivities and good stabilities [2]. The metallic alloys composed of aluminum (Al), copper (Cu), magnesium (Mg), silicon (Si), and zinc (Zn) had been extensively studied in the temperature range of 250–700°C. However, their volumetric latent heats are lower than 2 kJ·cm^{-3} [3–11].

Si stands out as a promising HTPCM, due to its high heat of fusion (4.09 kJ·cm^{-3}) [12], abundance, and low cost. However, its volume expansion during solidification (~10%) brings a significant hurdle to its application [13]. To overcome this limitation, Si is being mixed with boron (B) and iron (Fe) to create a Fe–Si–B eutectic alloy. This alloy is expected to have a similar heat of fusion and melting behavior to Si but with reduced volume expansion. The Fe–Si–B eutectic alloy's chemical composition was calculated to be 65 mass% Fe, 26 mass% Si, and 9 mass% B (Fe–26Si–9B) based on the FTlite database using FactSage 7.2 [14].

The thermodynamic and thermophysical properties of Fe–26Si–9B had been widely investigated [14–21]. The experimental results indicated that the alloy started to melt at ~1,220°C, and fully melted at ~1,254°C. The heat of fusion was measured to be ~3.7 kJ·cm^{-3}, which is slightly lower than that of pure Si [12] but higher than that of other known metallic eutectic alloys [3–11]. A slight volume shrinkage was

* **Corresponding author: Jianmeng Jiao,** Department of Materials Science and Engineering, Norwegian University of Science and Technology (NTNU), Trondheim N-7491, Norway,
e-mail: jian.m.jiao@ntnu.no
Sethulakshmy Jayakumari: Department of Metal Production and Processing, SINTEF Industry, Trondheim N-7491, Norway
Maria Wallin, Merete Tangstad: Department of Materials Science and Engineering, Norwegian University of Science and Technology (NTNU), Trondheim N-7491, Norway

observed during solidification, as anticipated. These findings suggest that Fe–26Si–9B alloy is a promising HTPCM that can be used at temperatures over 1,000°C. Additionally, thermal cycle experiments had been conducted in graphite crucibles at the laboratory scale [14–21]. The alloys were subjected to 1–16 thermal cycles in the melting/solidification process under argon (Ar). A continuous carbide layer was formed between the alloy and graphite crucibles, which served as a barrier layer to protect against the penetration of the molten alloy. No cracks were observed in the graphite crucible. Graphite is hence regarded as a potential refractory material for the Fe–26Si–9B alloy's container.

Based on these promising results, pilot-scale experiments are designed to be conducted using a specially shaped graphite crucible to test the high temperature part of the latent heat TES system [22]. The purpose is to investigate the phase distributions during thermal cycles, the interaction between Fe–26Si–9B master alloy and graphite, and the physical conditions of graphite crucible after thermal cycles. The outcomes of these pilot-scale experiments will provide crucial insights into the behavior of the high temperature part of the latent heat TES system under a more realistic operating condition.

2 Materials and methods

2.1 Raw materials

The Fe–26Si–9B master alloy was produced by mixing various raw materials, which is metallurgical grade (MG-grade) Si, Fe pieces, and FeB alloy. The MG-grade Si (>99 mass% Si) is in the form of lumps with a size range of 3–5 cm. Fe pieces (99.97 mass% Fe) is from Alfa Aesar with a size greater than 25 mm. FeB alloy (18.67 mass% B) is from GfE-MIR GmbH.

The raw materials (~6 kg) were placed in a graphite crucible and heated to 1,700°C. This heating process took place in an open furnace, which has a maximum power output of 75 kW. Notably, this charged graphite crucible was heated in air. Once melted, the homogeneous liquidus alloy was immediately cast into a conical frustum shaped graphite crucible (IG-15 [23]) in air, which is specially designed for the latent heat TES system. Figure 1 shows a visualization of the physical object and the measurement details.

The chemical composition of the produced Fe–26Si–9B alloy was analyzed from two samples. One is from the side of the solidified alloy, while another is from the middle of the solidified alloy. Fe and Si were analyzed by X-ray fluorescence (XRF). B was analyzed by Inductively Coupled Plasma Optical Emission Spectroscopy (ICP-OES). The detected and normalized results are listed in Table 1.

2.2 Thermal cycle experiments

The thermal cycle experiments were performed using the produced Fe–26Si–9B master alloys in the conical frustum shaped crucibles. An induction furnace was employed for the study. To investigate the phase distribution after each cycle and the interaction between alloy and graphite crucible, the Fe–26Si–9B alloy pieces were placed into the graphite crucible, followed by subjecting to 2–3 thermal cycles within a temperature range of 1,100–1,375°C in an air atmosphere. Subsequently, the charged crucible was cooled at an approximately rate of 12°C·min^{-1}. The temperature during the experiments was recorded using a C

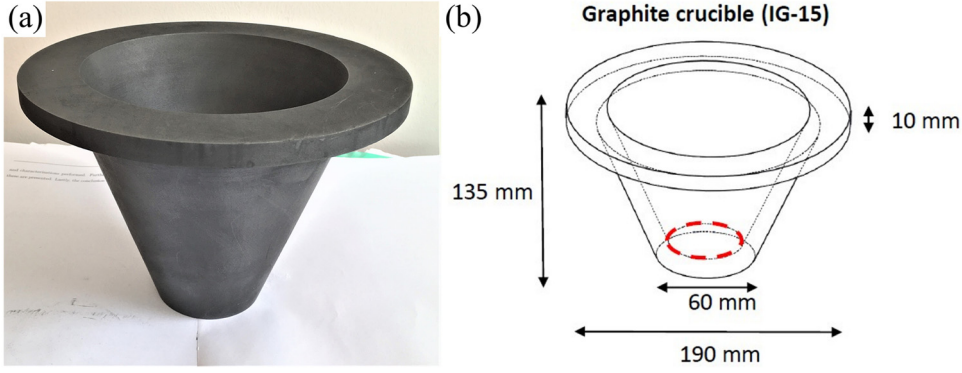

Figure 1: (a) Conical frustum shaped graphite crucible (IG-15) and (b) measurement details of the crucible.

Table 1: Chemical composition of the Fe–Si–B master alloy, Fe and Si were analyzed by XRF, and B was analyzed by ICP-OES (mass%)

Sample		Fe	Si	B
Fe–Si–B-side sample	Detected	65.0	26.0	8.9
	Normalized	65.1	26.0	8.9
Fe–Si–B-middle sample	Detected	65.0	26.0	9.2
	Normalized	64.9	25.9	9.2

type thermocouple, as illustrated in Figure 2. During the thermal cycle experiments, the Fe–26Si–9B samples were extracted from the middle position of the alloy at the molten state using either an alumina rod or graphite rod. Subsequently, the extracted samples were subjected to phase and chemical composition analyses.

To assess the potential for graphite crucible cracking subsequent to cooling to very low temperatures in thermal cycle experiments, a novel temperature profile had been implemented, as seen in Figure 3. This new temperature profile was designed to provide a more rigorous evaluation of the thermal stability and resistance to cracking of graphite crucible.

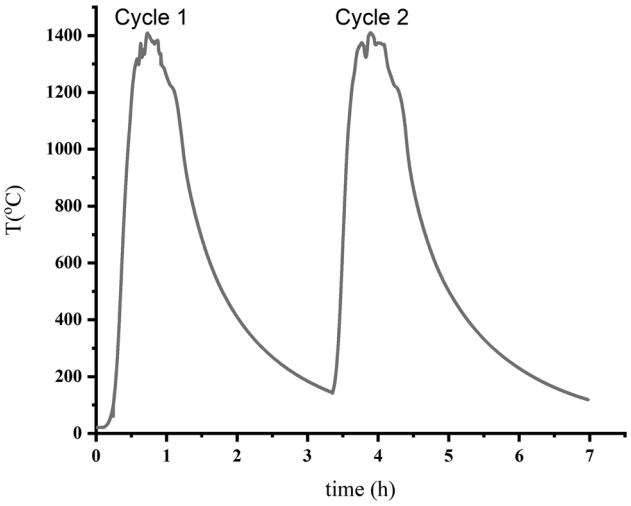

Figure 3: Temperature profile of thermal cycle experiment in the temperature range of 100–1,375°C.

2.3 Characterization

In this study, electron probe micro-analyzer (EPMA) is used to analyze the microstructures of samples. Furthermore, the chemical composition of the formed phase is determined through wavelength dispersive X-ray spectroscopy technique. ICP-OES is employed to analyze B content and XRF is used to analyze Fe and Si contents in the alloys. To predict the thermodynamic properties, FactSage software [24] is utilized, incorporating FTlite, FactPS, and FToxid databases in the calculation process.

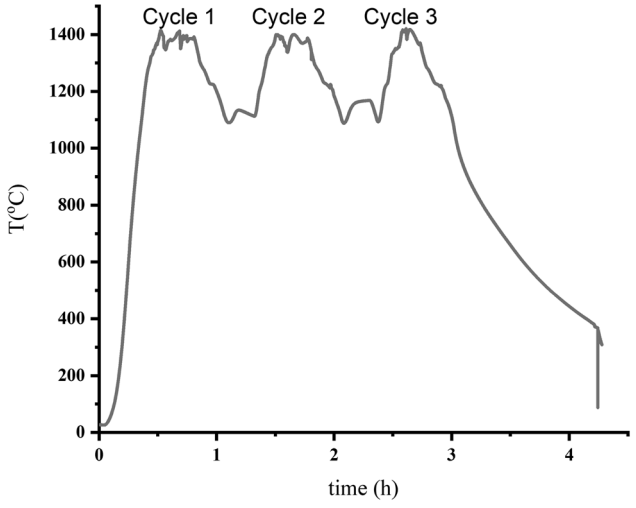

Figure 2: Temperature profile of thermal cycle experiments in the temperature range of 1,100–1,375°C.

3 Results and discussion

3.1 Phase distribution

The formed phases remain stable during thermal cycles in the temperature range of 1,100-1,375°C in the pilot-scale experiment in an open furnace. Figure 4a shows the phases formed in the master alloy. Figure 4b–d show the formed phases during thermal cycles, where the samples were extracted using an alumina rod at 1,375°C. It is seen from Figure 4 that FeB, FeSi, SiB_6, and $FeSiB_3$ were observed in the solidified alloys. Compared to the phases formed in the master alloy, it kept stable after 1–3 thermal cycles without introducing carbides. The phase distributions in the Fe–26Si–9B alloys had been extensively investigated in the lab-scale experiments under Ar [14–21]. In this studies, Grorud [14,17] performed the thermal cycle experiments in the graphite crucibles within 3–4 thermal cycles in the temperature range of 1,057–1,257°C, whereas Sellevoll [18] investigated the interaction of the alloy with graphite crucible under 16 long-term thermal cycles in the temperature range of 1,137–1,550°C. The thermal cycle experiments had also been conducted in the Si_3N_4 crucibles within 1-12 thermal cycles in the temperature range of 1,100–1,300°C [15]. From these studies, it was found that

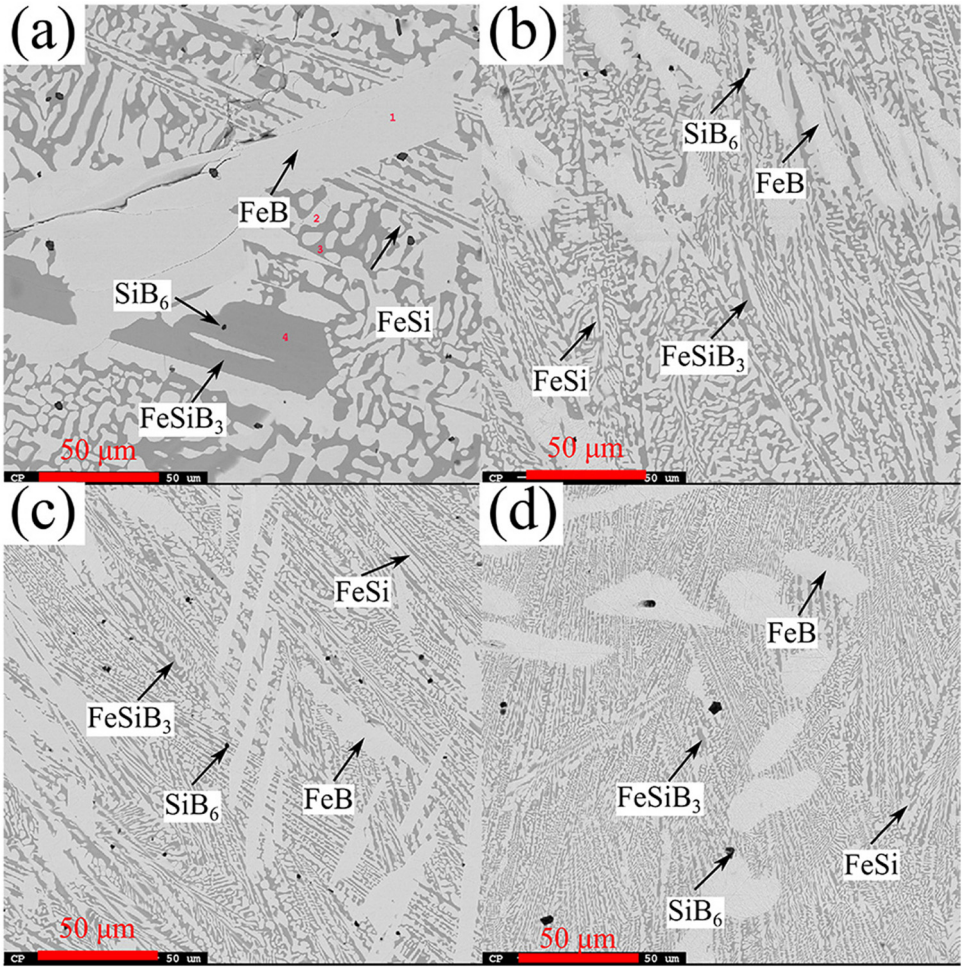

Figure 4: EPMA images of the solidified Fe–26Si–9B alloys: (a) master alloy used in the thermal cycle experiment, (b)–(d) the alloys taken out at 1,375°C in the first, second, and third cycles.

the phase distributions were identical to those produced in the pilot-scale experiment. This indicates that the phase distribution in the solidified Fe–26Si–9B alloys is independent of operating atmosphere and scale of the crucibles.

3.2 Effect of carbon impurity on Fe–Si–B alloy

SiC and B_4C precipitates are formed at the surface in the top position of the Fe–Si–B alloys. In order to investigate the effect of C impurity on the alloy, samples were extracted by dipping the graphite rod into the molten alloy during thermal cycles. Figure 5a shows the phase distribution in the Fe–Si–B alloy in the second cycle at 1,375°C. It is seen that SiC and B_4C were formed in the alloy. Interestingly, the B_4C particles were found to surround the SiC particles. Moreover, a thin SiC layer was formed at the interface between the graphite rod and the alloy. Figure 5b shows the microstructure at the surface in the top position of the solidified alloy. B_4C and SiC were detected in this area. Further investigations by Grorud [14,17] and Sellevoll [18] also showed that SiC and B_4C precipitates were formed at the surface of the alloy at the top position of the graphite crucible in lab-scale experiments, while no carbides were detected in the middle and bottom positions of the alloys after solidification. Therefore, it can be concluded that using graphite as a container in pilot-scale experiments is likely to result in the formation of SiC and B_4C precipitates at the surface of the alloys. The carbon solubility was estimated to be less than 0.3 mass% in the Fe–26Si–9B alloy at temperatures of 1,500–1,600°C [14]. During the cooling process, the dissolved carbon was expected to be precipitated into SiC particles, and then B_4C would be generated as the temperature decreased further. So, the chemical composition of

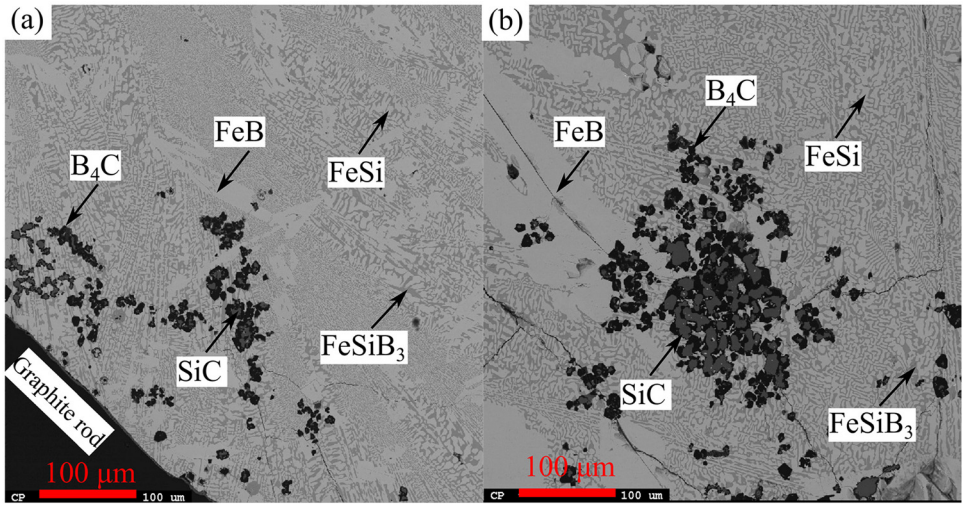

Figure 5: EPMA images of Fe–26Si–9B alloy: (a) the sample was extracted by the graphite rod at 1,375°C at the 2nd cycle, and (b) the sample was collected at the surface in the top position of the solidified alloy.

Fe–Si–B alloy would not have significant variations by introducing carbon.

The impact of carbon on the alloy's chemical composition is also investigated in the thermal cycle experiment, where five samples were continuously extracted by the graphite rod in the temperature range of 1,277–1,370°C. The resulting chemical compositions of B, Fe, and Si are summarized in Figure 6. It is found that B was in the range of 8.2–8.6 mass%, Fe was in the range of 64.2–67.2 mass%, and Si was in the range of 24.1–27.5 mass%. This showed that Fe and Si were similar to those of the master alloys. The B content was slightly lower than that of the master alloys, mainly due to the formation of carbides in the samples.

In the use of Fe–26Si–9B alloy in a graphite container for TES applications, the alloy goes through phase changes to store and release energy. The formed phases, including FeSi, FeB, $FeSiB_3$, and SiB_6, are stable throughout this process. Carbides are observed at the surface of the alloy at the top position during solidification. The chemical composition of the alloy remains relatively stable in the thermal cycle process. It shows the potential suitability of Fe–26Si–9B alloy as a PCM in TES system.

3.3 Interaction between Fe–Si–B alloy and graphite crucible

The interaction between Fe–26Si–9B alloy and graphite crucible has been investigated by analyzing the microstructures of four different regions of the graphite crucible, as shown by the red circles in Figure 7. It should be mentioned that the Fe–26Si–9B alloy falls out smoothly of the graphite crucible after solidification. The corresponding EPMA images are shown in Figure 8. It is seen that a white layer was produced between the Fe–26Si–9B alloy and graphite crucible. The width of this continuous white layer was measured in the range of 10–100 μm. Figure 9 shows the elemental distribution of the interlayer at position (d) in Figure 7. It is seen that the white layer consisted of a mixture of oxygen (O), calcium (Ca), silicon (Si), aluminum (Al), and sodium (Na). An oxide layer was formed between the Fe–26Si–9B alloy and graphite crucible in the thermal cycle experiment. This oxide layer was composed of CaO, SiO_2, Al_2O_3, and Na_2O, where these active elements originated from the charged raw materials. This can be attributed to the fact that Ca, Al, and Na exhibit greater activity with oxygen than Si. However, previous investigations into the interaction between Fe–26Si–9B alloy and graphite crucible had been performed under Ar in a closed system [14,17–21], and the results showed that a continuous layer of carbides (SiC + B_4C) was formed at the interface, this layer was also observed at the interface between the graphite rod and the Fe–Si–B alloy. So, when encountering O_2, an oxide layer was produced surrounding the Fe–Si–B alloy instead of carbides layer.

In the Fe–Si–B alloys, the formation of SiC and B_4C was also caused by the reaction of Si, B and C at the interface:

$$Si(l) + C(s) = SiC(s), \quad (1)$$

$$4B(l) + C(s) = B_4C(s). \quad (2)$$

Therefore, the Gibbs energy can be expressed as follow:

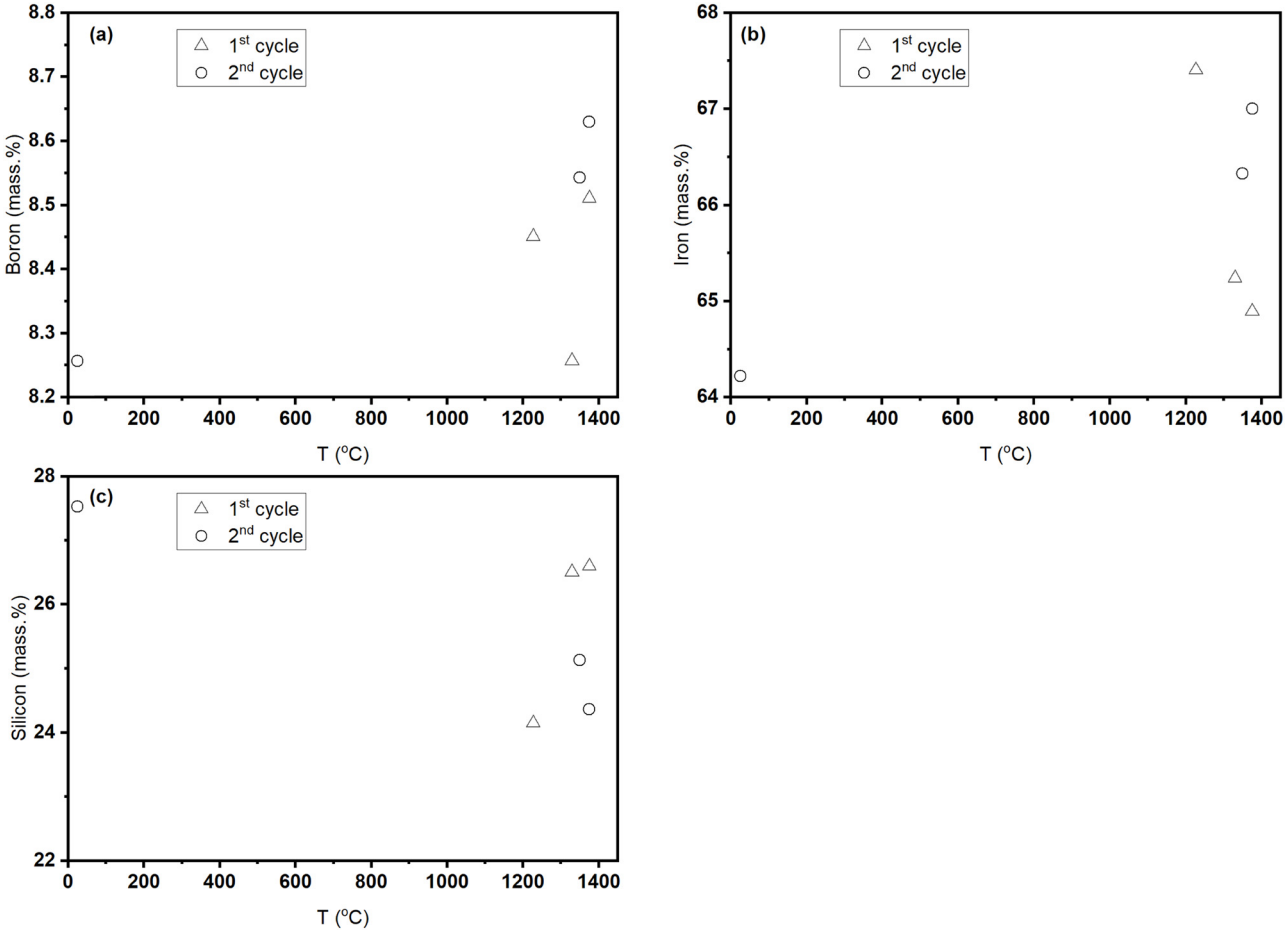

Figure 6: Chemical composition of Fe–26Si–9B alloy during thermal cycle experiment in the temperature range of 1,100–1,375°C: (a) B was analyzed by ICP-OES, (b) and (c) Fe and Si were analyzed by XRF.

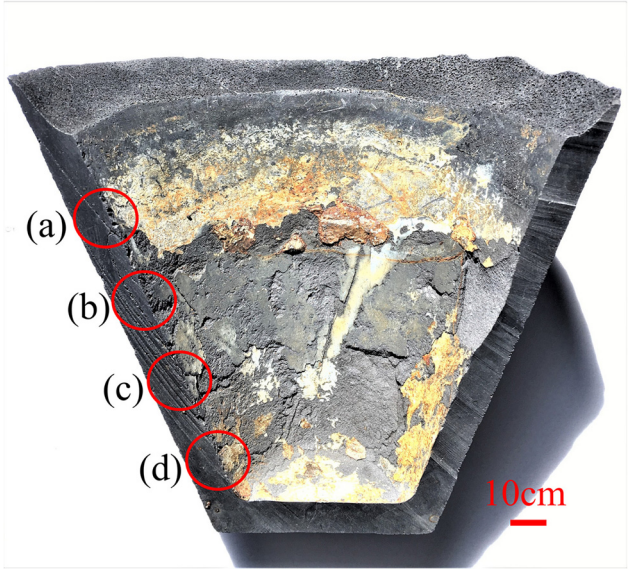

Figure 7: The cross section of the graphite crucible after two thermal cycles, and (a)–(d) present the corresponding sample positions for EPMA analyses.

$$\Delta G_{SiC} = \Delta G^0_{SiC} + RT \ln \frac{a_{SiC(s)}}{a_{C(s)} \cdot a_{Si(l)}}, \quad (3)$$

$$\Delta G_{B_4C} = \Delta G^0_{B_4C} + RT \ln \frac{a_{B_4C(s)}}{a_{C(s)} \cdot a_{B(l)}^4}, \quad (4)$$

where, $\Delta G_{SiC}{}^0$ and $\Delta G_{B4C}{}^0$ are constants at a given temperature, and they can be directly obtained from the FTlite databases. The values of $a_{SiC(s)}$, $a_{B4C(s)}$, and $a_{C(s)}$ are all unity. Hence, the Gibbs energies of SiC and B_4C can be calculated by knowing the activities of Si and B in the molten alloys.

Figure 10a shows the calculated activities of B and Si in the molten Fe–26Si–9B alloys at 1,200–1,550°C. Thus, the Gibbs energies of the formation of SiC and B_4C are calculated, as shown in Figure 10b. It is seen that the Gibbs energies for the formation of SiC and B_4C are negative, indicating that the reactions occur spontaneously. However, the Gibbs energy of B_4C formation is more negative than the Gibbs energy of SiC formation. It implies that the formation of B_4C is more favorable than SiC in the Fe–26Si–9B/graphite system.

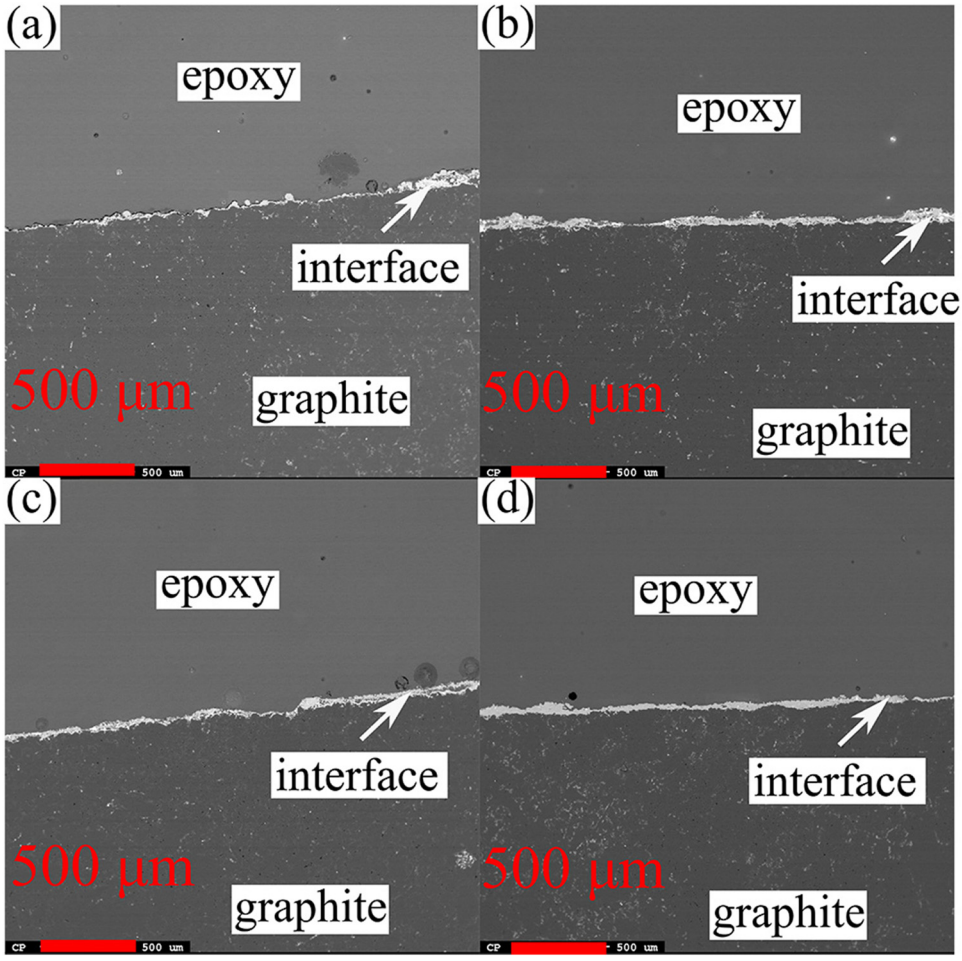

Figure 8: The interlayer between the Fe–26Si–9B alloy and graphite crucible at 4 different positions after 2 thermal cycles in the temperature range of 1,100–1,375°C. (a)–(d) corresponds to the positions in Figure 7.

In the use of graphite as a container for the Fe–26Si–9B alloy in the TES system in an open furnace, an oxide layer was formed between the alloy and graphite. This layer can act as a barrier layer to prevent the penetration of molten alloy into the graphite. As seen Figure 8, no penetration was observed in the graphite part. The alloy was slipping the graphite crucible after solidification, indicating a non-wetting behavior between the Fe–26Si–9B alloy and the oxide layer. However, in the presence of O_2, both the SiO_2 oxide layer and graphite will persistently consume O_2, consequently releasing SiO and CO gas. Over an extended duration, this process can alter the composition of the Fe–26Si–9B alloy and cause degradation to the graphite container.

3.4 Testing for crucible cracks

No cracks are observed in the graphite crucible after undergoing extreme temperature changes, where the Fe–26Si–9B alloy was subjected to two thermal cycles in the temperature range of 1,100–1,375°C in an induction furnace. Prior to the experiment, the top part of the conical frustum shaped crucible was cut at a length of 2–3 cm to fit the size of the induction furnace, as shown in Figure 11a. Figure 11b shows the graphite crucible after thermal cycle experiment, which showed no observed cracks. In the lab-scale experiments, it had demonstrated that the graphite crucible was capable of withstanding 1–17 thermal cycles in the melting/solidification process [14–21]. In the pilot-scale experiments, the Fe–26Si–9B alloy had also undergone 2–3 thermal cycles in the temperature range of 1,100–1,375°C. The graphite crucible remains intact after the experiments, even though with the cooling to very low temperatures. These results suggest that graphite crucible is generally reliable and can withstand phase changes without cracking. The present experimental result provides insight into the possibility of using a graphite crucible in fast temperature change conditions.

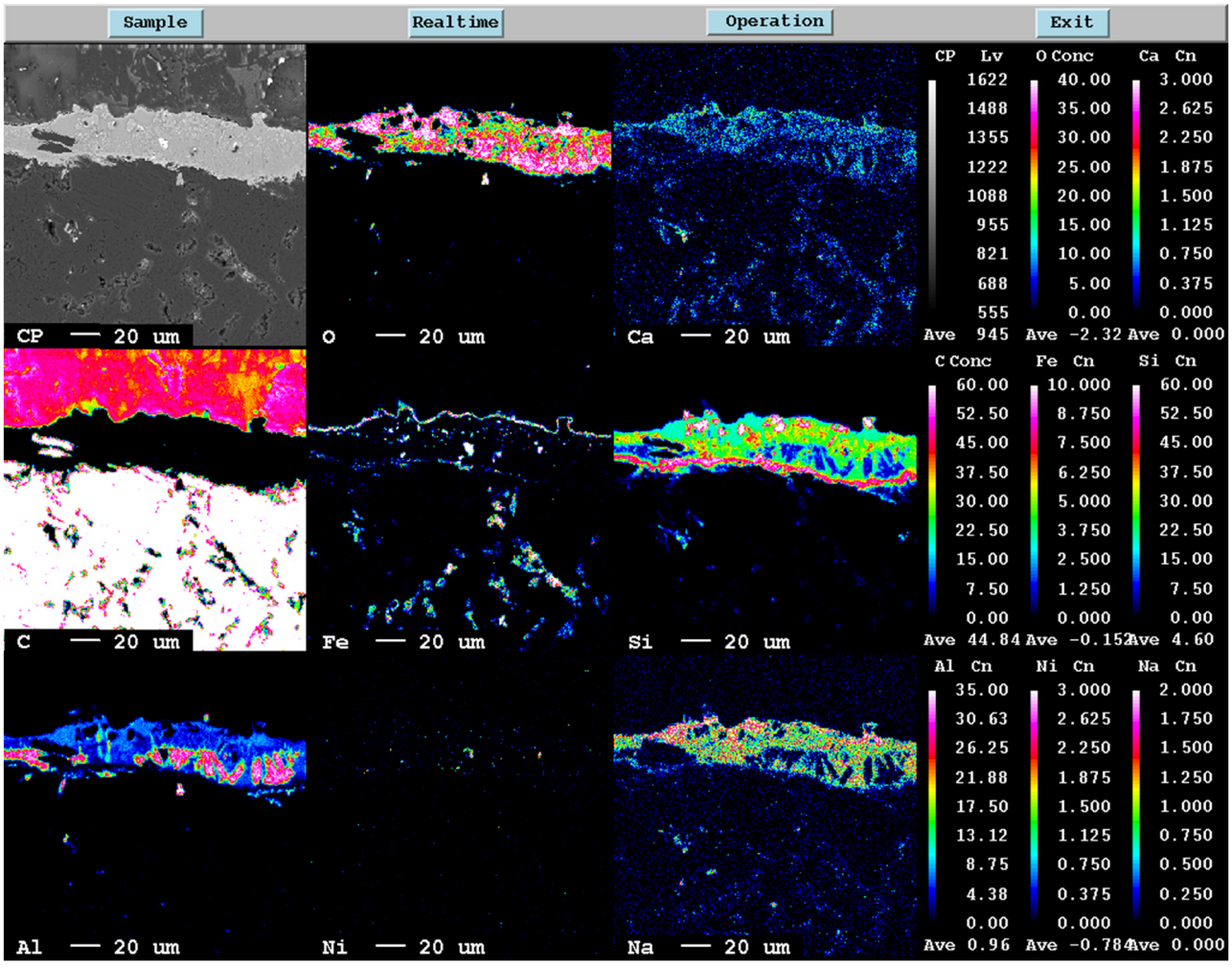

Figure 9: EPMA elemental map at the interface between the Fe–26Si–9B alloy and graphite crucible after two thermal cycles in the temperature range of 1,100–1,375°C.

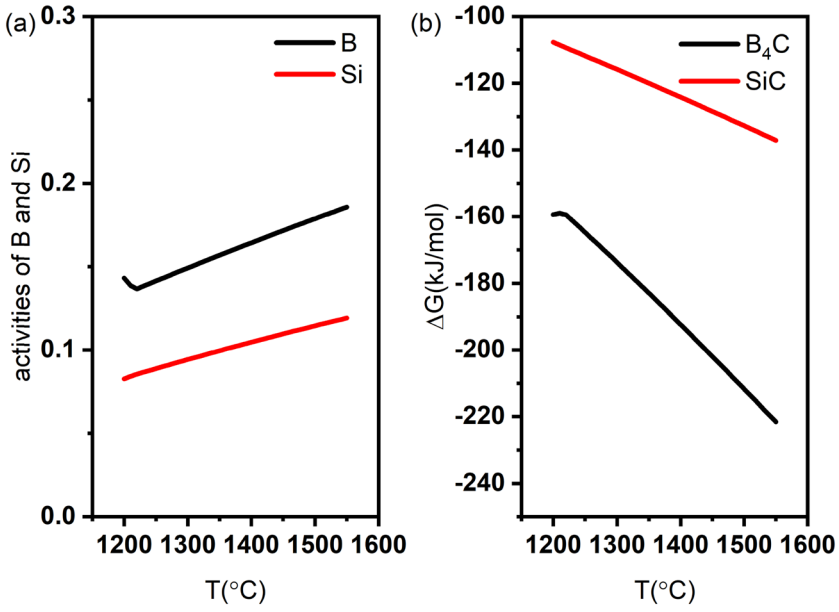

Figure 10: (a) The calculated activities of B and Si vs temperature in the Fe–26Si–9B alloys, and (b) the calculated Gibbs energies in the formation of B_4C and SiC vs temperature in the Fe–26Si–9B-C system. Calculated with FactSage 8.1 based on the FTlite and FactPS databases.

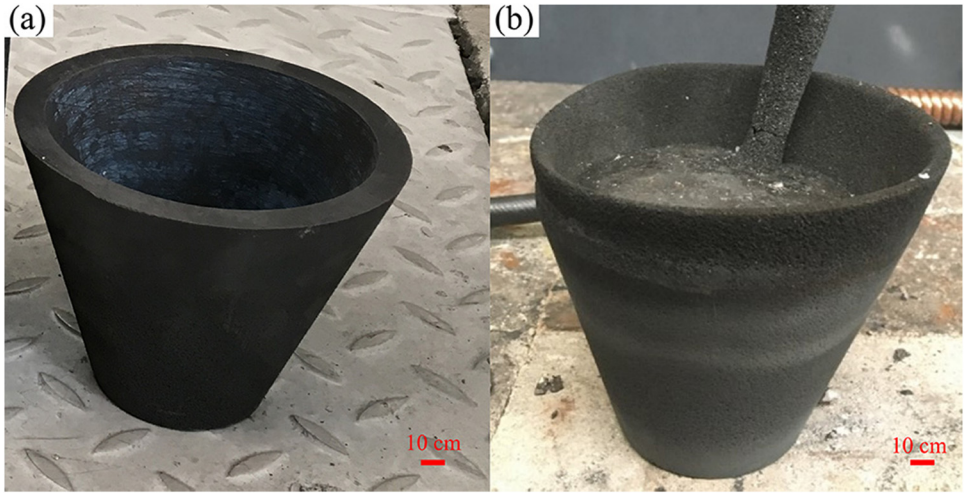

Figure 11: (a) Graphite crucible before thermal cycle experiment, (b) graphite crucible after two thermal cycles in the temperature range of 100–1,375°C.

4 Conclusions

The work aims to evaluate the possibility of using graphite material as a container for Fe–26Si–9B PCM in a pilot scale. 4–5 kg master alloys are placed in a graphite crucible, and then, it undergoes 2–3 thermal cycles in an induction furnace under an air atmosphere. According to the experimental results, the use of graphite as a container for Fe–26Si–9B PCM is a promising approach. However, it should be used in an inert atmosphere. The conclusions are summarized as follows.

1. The Fe–26Si–9B alloy remains stable after undergoing 2–3 thermal cycles.
2. SiC and B_4C precipitates are formed and exist at the surface of the solidified Fe–Si–B alloys.
3. The chemical composition of the Fe–26Si–9B alloy remains relatively stable during the thermal cycles.
4. In the presence of O_2, an oxide interlayer is formed between the Fe–26Si–9B alloy and graphite crucible after thermal cycle experiments. However, this process is accompanied by the release of SiO and CO gas.
5. Graphite crucible can withstand extreme temperature changes without cracking.

Acknowledgements: The THERMOBAT project received funds from European Commission under grant agreement 10105754. The sole responsibility for the content of this publication lies with the authors. It does not necessarily reflect the opinion of the European Union. Neither the REA nor the European Commission is responsible for any use that may be made of the information contained therein.

Funding information: This study was supported by the THERMOBAT project received funds from European Commission under grant agreement 10105754.

Author contributions: Jianmeng Jiao: writing – original draft, methodology; Sethulakshmy Jayakumari: investigation, methodology, formal analysis; Maria Wallin: writing – review and editing, supervision; Merete Tangstad: conceptualization, funding acquisition, writing – review and editing, supervision, project administration.

Conflict of interest: The authors declare no conflict of interest.

Data availability statement: Data would be available with the permission by the THERMOBAT project under grant agreement 10105754.

References

[1] IEA World Energy Outlook. Paris: 2019, Vol. 2019.
[2] Magomedov, A. M. Netraditsionnye Istochniki Energii (Non-Traditional Sources of Energy), 1996.
[3] Kotzé, J. P. P., T. W. W. von Backström, and P. J. J. Erens. Simulation and testing of a latent heat thermal energy storage unit with metallic phase change material. In: *Proceedings of the Energy Procedia*, Elsevier: January 1 2013, Vol. 49, pp. 860–869.
[4] He, Q. and W. Zhang. A study on latent heat storage exchangers with the high-temperature phase-change material. *International Journal of Energy Research*, Vol. 25, 2001, pp. 331–341.
[5] Akiyama, T., Y. Ashizawa, and J. Yagi. Storage and release of heat in a single spherical capsule containing phase change material of

high melting point. *Heat Transfer Japanese Research*, Vol. 21, 1992, pp. 199–217.
[6] Li, F., Y. J. Hu, and R. Y. Zhang. The influence of heating-cooling cycles on the thermal storage performances of Al-17 Wt.% Si alloy. *Advanced Materials Research*, Vol. 239–242, 2011, pp. 2248–2251.
[7] Kotzé, J. P., T. W. Von Backström, and P. J. Erens. High temperature thermal energy storage utilizing metallic phase change materials and metallic heat transfer fluids. *Journal of Solar Energy Engineering, Transactions of the ASME*, Vol. 135, 2013, id. 035001.
[8] Khare, S., M. Dell'Amico, C. Knight, and S. McGarry. Selection of materials for high temperature latent heat energy storage. *Solar Energy Materials and Solar Cells*, Vol. 107, 2012, pp. 20–27.
[9] Cárdenas, B. and N. León. High temperature latent heat thermal energy storage: Phase Change materials, design considerations and performance enhancement techniques. *Renewable and Sustainable Energy Reviews*, Vol. 27, 2013, pp. 724–737.
[10] Farkas, D. and C. E. Birchenall. New Eutectic alloys and their heats of transformation. *Metallurgical Transactions A*, Vol. 16, 1985, pp. 323–328.
[11] Gasanaliev, A. M. and B. Y. Gamataeva. Heat-Accumulating Properties of Melts. *Russian*. *Chemical Reviews*, Vol. 69, 2000, pp. 179–186.
[12] Zaitsev, A. I. and A. A. Kodentsov. Thermodynamic Properties and Phase Equilibria in the Si-B System. *Journal of Phase Equilibria*, Vol. 22, 2001, pp. 126–135.
[13] Rhim, W. K. and K. Ohsaka. Thermophysical properties measurement of molten silicon by high-temperature electrostatic levitator: Density, volume expansion, specific heat capacity, emissivity, surface tension and viscosity. *Journal of Crystal Growth*, Vol. 208, 2000, pp. 313–321.
[14] Jiao, J., B. Grorud, C. Sindland, J. Safarian, K. Tang, K. Sellevoll, et al. The use of Eutectic Fe–Si–B alloy as a phase change material in thermal energy storage systems. *Materials*, Vol. 12, 2019, id. 2312.
[15] Jiao, J., J. Safarian, and M. Tangstad. The use of Fe–26Si–9B alloy as phase change material in Si3N4 container. *Crystals*, Vol. 12, 2022, id. 376.
[16] Jiao, J. M., B. Grorud, J. Safarian, and M. Tangstad. Wettability of molten Fe–Si–B alloy on graphite, Al2O3, and h-BN substrates. In: *Proceedings of the Liquid Metal Processing & Casting Conference*, Vol. 2019, 2019, pp. 425–433.
[17] Grorud, B. Interaction of Eutectic Fe–Si–B alloy with graphite crucibles. *Master Thesis*, Norwegian University of Science and Technology, Trondheim, 2018.
[18] Sellevoll, K. *Interactions of Eutectic Fe–Si–B Alloy with Graphite Crucibles*, NTNU, Trondheim, 2018.
[19] Sellevoll, K. Interactions of FeSi alloys with graphite crucibles. *Master Thesis*, Norwegian University of Science and Technology, Trondheim, 2019.
[20] Sindland, C. *Production of Eutectic Si–Fe–B and Si–Cr–B Alloy and Their Interaction with Graphite Crucibles*, Norwegian University of Science and Technology, Trondheim, 2018.
[21] Jiao, J. M. Si-based phase change materials in thermal energy storage systems. *Ph.D Thesis*: NTNU, 2020.
[22] Datas, A., A. López-Ceballos, E. López, A. Ramos, and C. del Cañizo. Latent heat thermophotovoltaic batteries. *Joule*, Vol. 6, 2022, pp. 418–443.
[23] Toyo Tanso Co. Ltd. Special Graphite (Isotropic Graphite), https://www.toyotanso.com/Products/Special_graphite/.
[24] FactSage The Integrated Thermodynamic Databank System, http://www.factsage.com/fs_general.php.